# Environmental Science & Technology

Iron(III)-Bearing Clay Minerals Enhance Bioreduction of Nitrobenzene by *Shewanella putrefaciens* CN32

Fubo Luan, Yan Liu, Aron M. Griffin, Christopher A. Gorski, and William D. Burgos*

Department of Civil and Environmental Engineering, The Pennsylvania State University, University Park, Pennsylvania 16801-1408, United States

Ⓢ *Supporting Information*

ABSTRACT: Iron-bearing clay minerals are ubiquitous in the environment, and the clay−Fe(II)/Fe(III) redox couple plays important roles in abiotic reduction of several classes of environmental contaminants. We investigated the role of Fe-bearing clay minerals on the bioreduction of nitrobenzene. In experiments with *Shewanella putrefaciens* CN32 and excess electron donor, we found that the Fe-bearing clay minerals montmorillonite SWy-2 and nontronite NAu-2 enhanced nitrobenzene bioreduction. On short time scales (<50 h), nitrobenzene reduction was primarily biologically driven, but at later time points, nitrobenzene reduction by biologically formed structural Fe(II) in the clay minerals became increasingly important. We found that chemically reduced (dithionite) iron-bearing clay minerals reduced nitrobenzene more rapidly than biologically reduced iron-bearing clay minerals despite the minerals having similar structural Fe(II) concentrations. We also found that chemically reduced NAu-2 reduced nitrobenzene faster as compared to chemically reduced SWy-2. The different reactivity of SWy-2 versus NAu-2 toward nitrobenzene was caused by different forms of structural clay-Fe(II) in the clay minerals and different reduction potentials (E_h) of the clay minerals. Because most contaminated aquifers become reduced via biological activity, the reactivity of biogenic clay−Fe(II) toward reducible contaminants is particularly important.
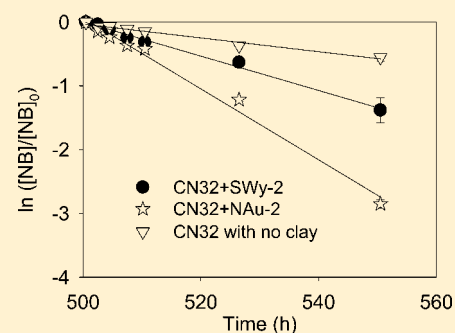
■ INTRODUCTION

Iron-bearing clay minerals are widely distributed in nature and have been estimated to account for up to 50% of the Fe in soils and sediments.[1−3] Much of the structural Fe in clay minerals can participate in redox reactions,[4] and the Fe(II)/Fe(III) redox couple is thought to be an important redox buffer across a wide range of redox conditions.[5−16] Structural Fe(II) in clay minerals is also important from an environmental perspective since it can reduce a wide range of contaminants, including toxic metals,[17,18] radionuclides,[19−21] nitroaromatic explosives,[22−24] and chlorinated solvents,[25] altering their fate and mobility. Structural Fe(III) in clay minerals can be reduced both abiotically, for instance by dissolved Fe(II), sulfide, and reduced natural organic matter,[26,27] and biotically by several types of naturally occurring metal- and sulfate-reducing microorganisms.[28,29]

Nitroaromatic compounds (NACs) are ubiquitous environmental contaminants. Understanding the environmental fate of NACs is of great interest due to their mutagenic and carcinogenic effects.[30,31]

The abiotic reduction of NACs by chemically reduced iron-bearing clay minerals has been well studied.[22−24] Several types of dissimilatory metal-reducing bacteria (DMRB) can reduce both NACs[32,33] and iron-bearing clay minerals.[34,35] As noted in a recent review, what remained unclear was if and how iron-bearing clay minerals would influence the bioreduction of NACs by DMRB.[36] In these systems, clay−Fe(III) reduction may compete with NAC reduction for available electron donor, and/or produce biogenic structural clay−Fe(II) that serves as a reductant of the NAC.

In previous work, we examined interactions between hematite, nitrobenzene, and *Shewanella putrefaciens* CN32, a DMRB capable of using both hematite and nitrobenzene as terminal electron acceptors.[32] In that system, Fe(II)-mediated reduction of nitrobenzene enhanced the rate of nitrobenzene reduction. However, nitrobenzene reduction occurred primarily by direct respiration by DMRB on short time scales (<24 h). We suggested that Fe(II)-mediated reduction by iron oxides would become a more important role on bioreduction of nitrobenzene in long-term experiments. Iron-bearing clay minerals differ from iron oxides in many ways.[37,38] Importantly, the content and structural locations of iron in clay minerals are distinct from oxides. Additionally, the reduction of iron-bearing clay minerals is not subject to reductive dissolution to the same extent as with iron oxides.[39] Therefore, we were interested in the interactions between iron-bearing clay minerals, DMRB, and nitrobenzene. We anticipated that our new findings would differ from previous work done with iron oxides, and purposefully conducted long-term experiments to differentiate short-term and long-term effects.

Many studies examining contaminant reduction by structural Fe(II) in clay minerals use chemically reduced specimens.[22−24]

Fe(III)-bearing clay minerals reduced by microorganisms versus chemical reductants yield products that are different with respect to their spectroscopic properties.[40] This has led to the suggestion that bacteria and commonly used chemical reductants reduce structural Fe(III) via different reaction mechanisms, and that the clay-microbe interactions may involve more than just electron transfer.[40] To date, we know of no studies that have compared the reactivity of biologically reduced versus chemically reduced iron-bearing clay minerals with NACs. Such knowledge is particularly important to the natural attenuation of NACs.

In the current work, we examined the role of iron-bearing clay minerals on the bioreduction of NACs by DMRB. To study these interactions, we (i) used nitrobenzene as a model NAC contaminant since it has been used extensively in the past to probe the reductive capabilities of Fe(II)-bearing clay minerals in abiotic systems;[22−24] (ii) selected montmorillonite SWy-2 (0.40 mmol Fe/g) and nontronite NAu-2 (4.1 mmol Fe/g) as two model clay minerals because they represent smectite end-members with respect to Fe content[20]; and (iii) chose *Shewanella putrefaciens* CN32 as a model Fe-reducing bacterium since it can respire on both clay−Fe(III) and nitrobenzene. In long-term bioreduction experiments, nitrobenzene was respiked into the batch reactors multiple times to gauge the importance of biotic versus abiotic nitrobenzene reduction with increasing concentrations of clay-Fe(II). Abiotic nitrobenzene reduction experiments were also conducted with biologically reduced (and pasteurized) and chemically reduced clay minerals to examine how the Fe(III) reduction pathway influenced the reactivity of clay−Fe(II).

■ MATERIALS AND METHODS

Microorganism and Culture Conditions. *Shewanella putrefaciens* strain CN32 was grown aerobically on tryptic soy broth without dextrose (Difco) at 20 °C, and cells were harvested and prepared anaerobically as previously described.[32,41]

Minerals and Chemicals. Both nontronite NAu-2 and montmorillonite SWy-2 were purchased from the source clays repository of the Clay Minerals Society (West Lafayette, IN). The solid-phase mineral compositions of NAu-2[42] and SWy-2[20] have previously been reported as

NAu-2: $M^+_{0.72}$ -$[Si_{7.55}Al_{0.16}Fe_{0.29}][Al_{0.34}Fe_{3.54}Mg_{0.05}]O_{20}(OH)_4$, where M may be Ca, Na or K

SWy-2: $(Ca_{0.16}Na_{0.24})$-$[Si_{6.73}Al_{1.27}][Al_{1.45}Fe^{2+}_{0.01}Fe^{3+}_{0.12}Mg_{0.44}]$-$O_{20}(OH)_4$

NAu-2 and SWy-2 were suspended in 0.5 M NaCl for 24 h, then separated by centrifugation, yielding the 0.5−2.0 μm clay size fraction. The clay fraction was washed with distilled deionized water (Milli-Q) repeatedly until no Cl$^-$ was detected by silver nitrate and then dried at 60 °C. Based on an anoxic HF-H$_2$SO$_4$/phenathroline digestion,[43] the NAu-2 clay fraction contained 4.1 mmol of Fe/g clay and 99.4% Fe(III), while the SWy-2 clay fraction contained 0.40 mmol of Fe/g clay and 97.3% Fe(III). NAu-2 and SWy-2 clay fraction stock solutions (20 g L^{-1}) were prepared in anoxic 10 mM PIPES [piperazine-N,N′-bis(2-ethanesulfonic acid), pK_a = 6.8] buffer adjusted to pH 6.8. Aluminum oxide (Al$_2$O$_3$) was used as a redox-inactive mineral control and its stock solution (20 g L^{-1}) was prepared in anoxic 10 mM PIPES buffer (pH 6.8).

Reagent grade nitrobenzene (Sigma-Aldrich), nitrosobenzene (TCI America), phenylhydroxylamine (Sigma-Aldrich), and aniline (Sigma-Aldrich) were used to prepare 0.16 M stock solutions in methanol.

Bioreduction of Iron(III)-Bearing Clay Minerals and Nitrobenzene. All experiments were conducted in 30 mL serum bottles crimp-sealed with Teflon-faced rubber stoppers. All preparations were performed in an anoxic chamber (Coy, Grass Lakes, MI) supplied with a 95:5 N$_2$:H$_2$ gas mix. The anoxic chamber (<1 ppm$_v$ O$_2$) was in a 20 °C constant-temperature room. Reactors were filled with ∼20 mL of deoxygenated 10 mM PIPES buffer (pH 6.8) containing various combinations of CN32 (1 × 10^8 cell/mL), NAu-2 or SWy-2 or Al$_2$O$_3$ (2.0 g/L), and nitrobenzene (210 μM). Ten mM sodium lactate was provided as the electron donor for bioreduction experiments, a concentration high enough to reduce all the nitrobenzene and all the clay−Fe(III) in any experiment. Long-term experiments were conducted where nitrobenzene was respiked into the reactors (250 μM) at 45 and 500 h. Nitrobenzene concentrations were always less than 25 μM before nitrobenzene was respiked. Control reactors were prepared containing only nitrobenzene and buffer. Other sets of control reactors were prepared with CN32 and NAu-2 but without nitrobenzene plus 0.25% methanol (vol/vol %; to account for cosolvent addition) or nitrosobenzene (210 μM) or aniline (210 μM). Nitrosobenzene and aniline were included to examine the effects of nitrobenzene metabolites on clay-Fe(II) production. Methanol and aniline were shown to have no effect on clay−Fe(II) production (SI Figure S1). All treatments and controls were run in triplicate. Reactors were incubated at 100 rpm on orbital shakers within the anoxic chamber. After cell inoculation, samples were periodically removed with sterile needles and syringes. Samples were analyzed for soluble Fe(II), clay−Fe(II), and nitrobenzene and its metabolites as described below. All sampling and Fe(II) measurements were performed in the anoxic chamber.

Abiotic Reduction of Nitrobenzene by Reduced Iron(III)-Bearing Clay Minerals. Bioreduced clay minerals were prepared using CN32 and NAu-2 or SWy-2 (with no nitrobenzene) as described above. Reactors were incubated for 900 h, at which point the biogenic clay−Fe(II) concentration essentially stopped increasing. Cell-clay mineral suspensions were washed 3 times with anoxic 50 mM PIPES buffer (pH 6.8) to remove residual sodium lactate and were then pasteurized (75 °C for 60 min, three times over 5 days) to deactivate biological activity. No further attempt was made to remove spent biomass. The bioreduced clay minerals were prepared as stock solutions (20 g/L) in anoxic 50 mM PIPES buffer.

NAu-2 and SWy-2 were chemically reduced using sodium dithionite (6 g/L) in a sodium citrate (266 mM)/sodium bicarbonate (111 mM) buffer (CBD method).[44,45] These lower concentrations of dithionite and shorter reaction periods were used to produce partially reduced NAu-2. The chemically reduced clay minerals were washed 3 times with anoxic sodium citrate/sodium bicarbonate buffer and 3 times with anoxic 50 mM PIPES buffer to remove residual dithionite. Stock solutions (20 g/L) were prepared in anoxic 50 mM PIPES buffer.

Abiotic reduction of nitrobenzene was conducted with biologically reduced (and pasteurized) and chemically reduced clay minerals. Clay mineral suspension concentrations (g clay L^{-1}) were varied such that experiments began with equal clay−Fe(II) concentrations. For NAu-2, depending on the clay−Fe(III) reduction extent, clay suspension concentrations varied from 1.1 to 5.3 g L^{-1} and initial clay-Fe(II) concentrations ranged from 1.1 to 5.3 mM Fe(II). For SWy-2, clay suspension concentrations varied from 3.1 to 3.6 g L^{-1} and clay−Fe(II) concentrations ranged from 1.1 to 1.3 mM Fe(II). Nitrobenzene

was always added at a constant concentration of 250 μM. All treatments and controls were run in triplicate. Reactors were incubated at 100 rpm on orbital shakers within the anoxic chamber. Samples were periodically removed with sterile needles and syringes and analyzed for clay−Fe(II) and nitrobenzene as described below. Sample suspensions were centrifuged at 14 100g for 10 min (pelletized particles <0.02 μm) in the anoxic chamber. The supernatant was used to measure soluble Fe(II), nitrobenzene, nitrosobenzene, and aniline.

Analytical Methods. Nitrobenzene, nitrosobenzene, phenylhydroxylamine, and aniline were measured by an HPLC equipped with a C18 column and photodiode array detector using an methanol/water (1/1, v/v) mobile phase. Soluble Fe(II) was measured using the phenanthroline method.[46] The mineral pellet was used to measure the clay-Fe(II) concentration using a modified anoxic HF-H$_2$SO$_4$/phenanthroline digestion method.[43] Total clay-Fe(II) was calculated as the sum of the soluble Fe(II) plus HF-H$_2$SO$_4$/phenanthroline Fe(II).

Mössbauer Spectroscopy. Transmission Mössbauer spectroscopy was performed using a SVT400 cryogenic Mössbauer system (SEE Co.). The ^{57}Co (~50 mCi) was in a Rh matrix at room temperature. All hyperfine parameters were reported relative to α-Fe foil at room temperature. Clay mineral wet pastes were prepared anaerobically and sealed between two pieces of 5 mL kapton tape to avoid oxidation when the sample was transferred from the anoxic chamber to the sample holder. Spectral fitting was conducted using Recoil Software (University of Ottawa, Ottawa, Canada). All fits were done using a Voigt-based model. The Lorentzian line width was held at 0.14 mm s^{-1} during fitting, as it was the line width measured on the spectrometer for an ideally thick α-Fe foil. For all fits, unless otherwise noted, the center shift (CS), quadrupole shift (QS), and relative areas between sites were allowed to float during fitting.

Kinetic Analyses. The rate of nitrobenzene reduction by CN32 or clay-Fe(II) was modeled as pseudo-first-order with respect to the nitrobenzene concentration according to

$$-d[\text{nitrobenzene}]/dt = k_{\text{cells}} \times [\text{nitrobenzene}] \quad (1)$$

where k_{cells} is the first-order reduction rate constant (d^{-1}) used to denote the rate by CN32-only; $k_{\text{cells+clay}}$ is used to denote the first-order reduction rate constant by CN32 in the presence of iron-bearing clay minerals, and; k_{clay} is used to denote the first-order reduction rate constant by clay−Fe(II) in abiotic experiments.

To quantify electron transfer in our experiments, we calculated zero-order reaction rates normalized to electron equivalents. Reduction rates of nitrobenzene (R_{NB}) and clay−Fe(III) (R_{Fe}) were calculated as (μeq L^{-1} h^{-1})

$$R_{\text{NB}} = 6 \times [\text{aniline}_t]/t \quad (2)$$

$$R_{\text{Fe}} = ([\text{clay} - \text{Fe(II)}_t] - [\text{clay-Fe(II)}_0])/t \quad (3)$$

where [aniline$_t$] is the concentration of aniline at time t (μM), t is the length of the spike-period (h), [clay−Fe(II)$_t$] is the total Fe(II) concentration (HF−H$_2$SO$_4$/phenanthroline + soluble) at the end of the spike-period (μM), and [clay−Fe(II)$_0$] is measured at the start of the spike-period (μM). Zero-order rates were used because they fit the kinetics of both aniline and Fe(II) production (eqs 2 and 3, respectively) reasonably well over most of the spike-periods. Zero-order rates were also used to directly compare electron transfer to nitrobenzene versus clay−Fe(III) in biotic experiments, and electron transfer to nitrobenzene from

clay−Fe(II) in abiotic experiments. Reduction of nitrobenzene to aniline is known to be a six electron transfer process.[32,47] Therefore, electron equivalents were calculated by multiplying aniline concentrations and 6 e$^-$ per mol in eq 2. Aniline concentrations were used instead of nitrobenzene because they represented the final reduced product.

To quantitatively compare nitrobenzene reduction rates with and without an iron-bearing clay mineral, we define a "clay enhancement factor" as

$$\text{clay enhancement factor} = k_{\text{cells+clay}}/k_{\text{cells}} \quad (4)$$

All statistical analyses were performed using IBM SPSS Statistics 20 (IBM Corp. NY).

■ RESULTS AND DISCUSSION

Biological Reduction of Nitrobenzene. To test the role of iron-bearing clay minerals on the bioreduction of nitrobenzene by DMRB we used *Shewanella putrefaciens* CN32 to reduce (*i*) nitrobenzene in the presence/absence of iron-bearing clay minerals and (*ii*) iron-bearing clay minerals in the presence/absence of nitrobenzene. We found that *Shewanella putrefaciens* CN32 concurrently reduced both nitrobenzene and clay−Fe(III) (Figure 1a,d,g). After the first spike of nitrobenzene (Spike 1 in Figure 1), the first-order rate constant for nitrobenzene reduction (k_{cell}) was 1.31 ± 0.01 d^{-1} in the absence of clay, and increased to 1.88 ± 0.05 d^{-1} and 1.53 ± 0.01 d^{-1} in the presence of montmorillonite SWy-2 and nontronite NAu-2 ($k_{\text{cells+clay}}$), respectively (Figure 1a, Table 1). Both SWy-2 and NAu-2 significantly ($P < 0.01$) enhanced the kinetics of nitrobenzene reduction. Nitrobenzene reduction rates in the presence of Al$_2$O$_3$ were not significantly different from results obtained with CN32 alone ($P > 0.1$; SI Figure S2). This result indicated that the enhancement of nitrobenzene reduction by iron-bearing clay minerals was not solely attributed to the presence of a mineral surface, and that iron(II) in clay minerals likely played an important role in the enhancement of nitrobenzene reduction. Sorption of nitrobenzene to the clay minerals or Al$_2$O$_3$ did not account for more than 1% of the added mass of nitrobenzene in any of the experiments.

The clay enhancement factors (eq 4) were greater than one for both SWy-2 and NAu-2 and increased over time. The increased rate of nitrobenzene reduction in the presence of iron-bearing clay minerals was driven by biogenic clay−Fe(II). Nitrobenzene and clay−Fe(III) did not become competitive electron acceptors because excess electron donor was provided.[32] The production of biogenic clay-Fe(II) then promoted the abiotic reduction of nitrobenzene. We hypothesized that clay−Fe(II)-mediated reduction would become increasingly important with the accumulation of biogenic clay−Fe(II). To test this, we respiked nitrobenzene into the reactors two additional times (Spike 2 at t = 45 h, Spike 3 at t = 500 h). These experiments allowed us to assess how nitrobenzene fate was affected by extended incubation times and increased clay−Fe(II) concentrations. Each nitrobenzene spike resulted in its rapid reduction (Figure 1a−c). For all three spikes and with both clay minerals we observed faster nitrobenzene reduction when the clay mineral was present relative to only CN32. The clay enhancement factors increased with each sequential spike of nitrobenzene for both clay minerals (SWy-2: Spike 1 = 1.43 ± 0.03, Spike 2 = 1.89 ± 0.04, Spike 3 = 2.49 ± 0.14; NAu-2: Spike 1 = 1.17 ± 0.01,
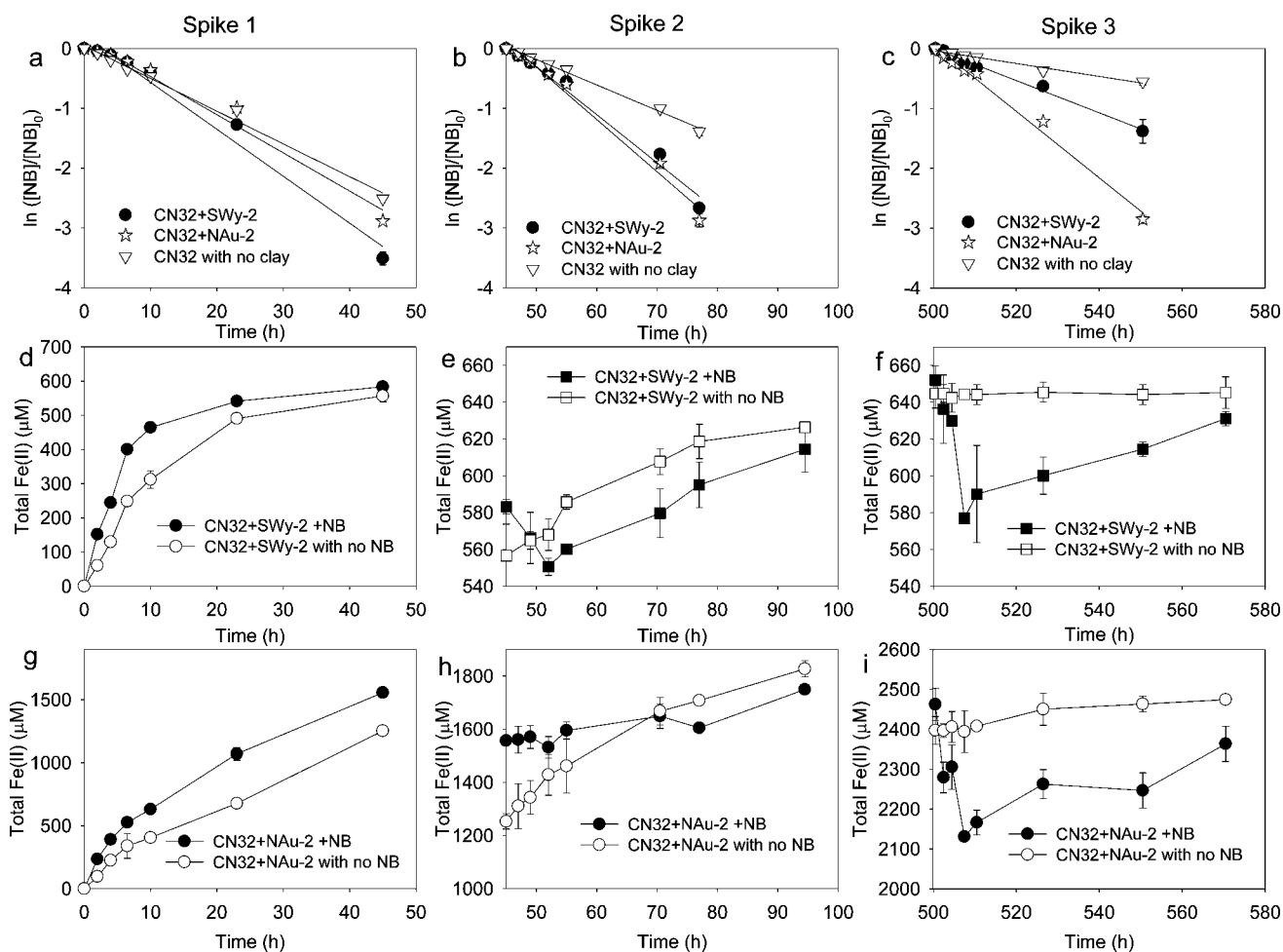
Figure 1. Biological reduction of nitrobenzene and iron-bearing clay minerals by *Shewanella putrefaciens* CN32. Experiments were initiated at $t = 0$ h with 210 μM nitrobenzene, 1.0×10^8 cell mL^{-1} CN32, 10 mM lactate and H$_2$ (2.5% headspace), and 2.0 g L^{-1} montmorillonite SWy-2 [0.78 mM clay–Fe(III)] or 2.0 g L^{-1} nontronite NAu-2 [8.2 mM clay–Fe(III)] in 10 mM PIPES buffer, pH 6.8. Nitrobenzene (250 μM) was re-spiked into the reactors at $t = 45$ h and $t = 500$ h. (a–c) ln([nitrobenzene]$_t$/[nitrobenzene]$_0$) versus time. (d–f) SWy-2 Fe(II) concentrations versus time. (g–i) NAu-2 Fe(II) concentrations versus time.

Spike 2 = 2.05 ± 0.05, Spike 3 = 5.14 ± 0.12; Table 1), thus, confirming our hypothesis.

Measurements of clay–Fe(II) concentrations over time further confirmed the role that clay–Fe(II) played in this process. Clay–Fe(II) concentrations steadily increased over the first 45 h of the experiment (Figure 1d,g), increased more slowly from 45 to 100 h (Figure 1e,h), and then remained unchanged or declined from 100 to 550 h (Figure 1f,i). These data provided clear evidence that CN32 was simultaneously respiring on both clay–Fe(III) and nitrobenzene. Higher concentrations of clay–Fe(II) were measured in the presence of nitrobenzene as compared to the nitrobenzene-free controls in Spike 1 (Figure 1d,g), which was counterintuitive as one would expect clay-Fe(II) to be consumed via nitrobenzene reduction. We believe that this result was caused by an analytical interference in which intermediates in the nitrobenzene reduction process reduced Fe(III) during the acidic clay mineral digestion (SI Figure S3). This analytical interference was only an issue at the start of the experiments (Spike 1) when the clay–Fe(III) concentrations were highest, and became less important as clay–Fe(III) concentrations decreased (Spikes 2 and 3). At the longest incubation times, after Spike 3, clay–Fe(II) concentrations were systematically higher in the absence of nitrobenzene (Figure 1f,i). Since

nitrobenzene was the only oxidant present in the system, the drop in clay–Fe(II) was attributed to nitrobenzene reduction by clay-Fe(II).

Mössbauer spectroscopy (MBS) was used to provide an additional measure of the extent of clay-Fe(III) reduction (Figure 2). Mössbauer spectra were collected for the biologically reduced minerals after 550 h of incubation to independently determine the clay-Fe(II) concentrations (Table 2). The values measured with Mössbauer spectroscopy were in reasonable agreement with those determined by HF–H$_2$SO$_4$/phenanthroline digestion. Clay-Fe(II) concentrations measured by HF–H$_2$SO$_4$/phenanthroline digestion were always higher than Fe(II) concentrations measured by MBS, except for one partially chemically reduced NAu-2 sample. Fe(II) concentrations measured by HF-H$_2$SO$_4$/phenanthroline digestion and MBS were in better agreement with NAu-2 versus SWy-2.

Electron Transfer Rates from CN32 to Nitrobenzene or Clay–Fe(III). Electron transfer rates from CN32 to clay–Fe(III) (R_{Fe}) and from CN32 to nitrobenzene (R_{NB}) were compared by normalizing the rates to the number of electrons transferred (eqs 2 and 3). The rate of nitrobenzene reduction by CN32 (in the absence of a clay mineral) was 25.5 μeq L^{-1} h^{-1} during Spike 1 (Table 1). The rate of clay–Fe(III) reduction by CN32 (in the absence of nitrobenzene) was

Table 1. Summary of Pseudo-First-Order Rate Constants for Nitrobenzene Reduction and Zero-Order Rates for Electron Transfer Reactions with Combinations of *Shewanella putrefaciens* CN32, Nitrobenzene, And Montmorillonite SWy-2 or Nontronite NAu-2.[a]

	experimental components			first-order rate constants k_{cells} or $k_{cells+clay}$ (d^{-1})[c] (R^2)[d]			electron transfer rates R_{NB} (μeq L^{-1} h^{-1})			R_{Fe} (μeq L^{-1} h^{-1})		
reaction description	nitrobenzene (μM)[b]	SWy-2 (g L^{-1})/ clay-Fe(III) (mM)	NAu-2 (g L^{-1})/ clay-Fe(III) (mM)	spike 1 0–45 h	spike 2 45–77 h	spike 3 500–550 h	spike 1 0–45 h	spike 2 45–77 h	spike 3 500–550 h	spike 1 0–45 h	spike 2 45–77 h	spike 3 500–550 h
nitrobenzene bioreduction	210–250	0/0	0/0	1.31 ± 0.01 (0.990)	1.02 ± 0.04 (0.995)	0.259 ± 0.03 (0.978)	25.5	33.9	10.5			
nitrobenzene reduction with SWy-2	210–250	2.0/0.78	0/0	1.88 ± 0.05 (0.977)	1.93 ± 0.01 (0.982)	0.646 ± 0.05 (0.992)	27.8	38.9	18.7	13.0	0.37	−0.75
nitrobenzene reduction with NAu-2	210–250	0/0	2.0/8.2	1.53 ± 0.01 (0.973)	2.10 ± 0.05 (0.983)	1.33 ± 0.04 (0.989)	26.1	41.9	24.6	34.6	1.50	−4.32
SWy-2 bioreduction	0	2.0/0.78	0/0							12.4	1.94	0.012
NAu-2 bioreduction	0	0/0	2.0/8.2							27.8	14.2	1.32

[a]All experiments conducted with 1×10^8 cells mL^{-1} CN32 and 10 mM lactate in 10 mM PIPES, pH 6.8. [b][Nitrobenzene]$_0$ = 210 μM at start of Spike 1. [nitrobenzene]$_0$ = 250 μM at starts of Spikes 2 and 3. [c]Regression slope ±95% confidence interval. [d]R^2 for regression of ln([nitrobenzene]$_t$/[nitrobenzene]$_0$) versus time of spike-period.
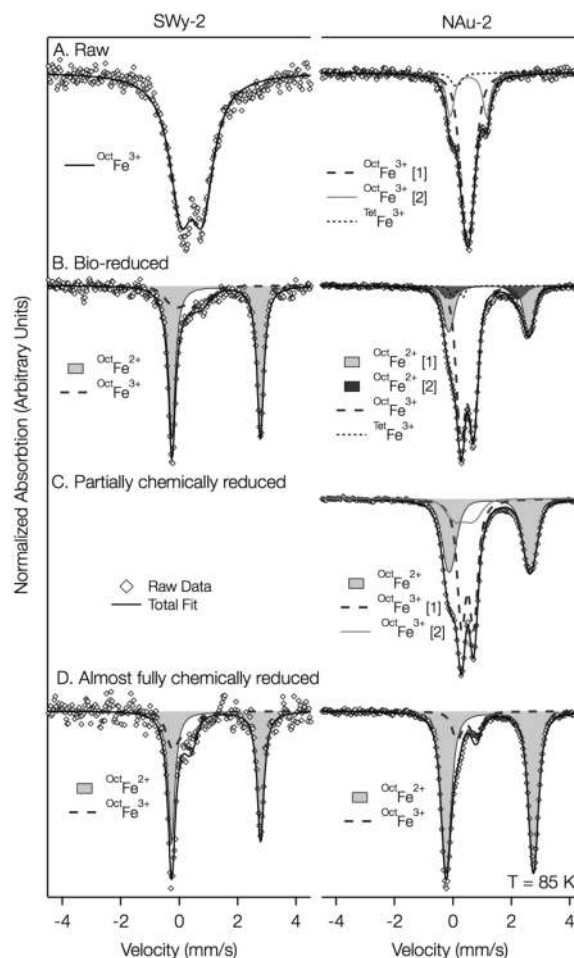
Figure 2. ^{57}Fe Mössbauer spectra collected for the native, biologically reduced and chemically reduced SWy-2 and NAu-2 samples at 85 °K. $^{Oct}Fe^{3+}$ = octahedral Fe(III), $^{Tet}Fe^{3+}$ = tetrahedral Fe(III), and $^{Oct}Fe^{2+}$ = octahedral Fe(II). Bracketed numbers shown after site assignments indicate that multiple distinct sites were found for the phase. Fitted hyperfine parameters and relative areas of each site are provided in Table 2.

12.4 μeq L^{-1} h^{-1} for SWy-2 and 27.8 μeq L^{-1} h^{-1} for NAu-2. The similarity between the values for nitrobenzene and NAu-2 suggested that CN32 could respire on nitrobenzene and clay−Fe(III) at nearly identical rates. The lower rate for SWy-2 relative to NAu-2 was due to the smaller amount of clay−Fe(III) in SWy-2.

Over longer incubation periods (Spikes 2 and 3 in Figure 1), CN32 reduced clay−Fe(III) at rates slower than for nitrobenzene (i.e., $R_{NB} \gg R_{Fe}$; Table 1). This was likely due to only a fraction of the remaining clay−Fe(III) being reducible due to biological accessibility and/or thermodynamic constraints.[35] Negative values for R_{Fe} during Spike 3 reflected the consumption of clay−Fe(II) coupled to nitrobenzene reduction. The reduction of nitrobenzene by clay−Fe(II) contributed to the high clay enhancement factors measured during Spike 3.

Abiotic Reduction of Nitrobenzene. In abiotic experiments, nitrobenzene was reduced by both bioreduced SWy-2 and bioreduced NAu-2 (Figure 3a,b). We found good stoichiometric agreement between 6 mol of Δclay−Fe(II) produced per 1 mol of Δaniline produced (Figure 3c). These results confirmed that Fe(III)-bearing clay minerals enhanced

E

Table 2. Mössbauer Spectroscopy (MBS) Fitted Hyperfine Parameters for Spectra Shown in Figure 2[a]

sample	CS, mm/s	QS, mm/s	phase	RA (%)	%Fe(II) by MBS	%Fe(II) by HF-H_2SO_4/phenanthroline
unaltered SWy-2	0.42	0.74	octahedral clay−Fe(III)	100.0	0	2.70
biologically reduced SWy-2	1.26	3.03	octahedral clay−Fe(II)	77.2	77.2	90.0
	0.27	0.87	octahedral clay−Fe(III)	22.8		
chemically reduced SWy-2	1.26	3.05	octahedral clay−Fe(II)	71.0	71.0	90.9
	0.07	0.61	octahedral clay−Fe(III)	29.0		
unaltered NAu-2	0.51	0.28	octahedral clay−Fe(III)	71.9	0	0.60
	0.52	1.25	octahedral clay−Fe(III) [2]	23.7		
	0.11	0.18	tetrahedral clay−Fe(III)	4.4		
biologically reduced NAu-2	1.06	2.33	octahedral clay−Fe(II)	8.5	32.3	34.5
	1.23	2.75	octahedral clay−Fe(II) [2]	23.8		
	0.48	0.44	octahedral clay−Fe(III)	64.5		
	0.16	0.35	tetrahedral clay−Fe(III)	3.2		
partially chemically reduced NAu-2	1.20	2.59	octahedral clay−Fe(II)	20.8	42.0	38.0
	1.27	2.96	octahedral clay−Fe(II) [2]	21.2		
	0.49	0.43	octahedral clay−Fe(III)	54.9		
	0..21	0.38	tetrahedral clay−Fe(III)	3.1		
chemically reduced NAu-2	1.26	2.99	octahedral clay−Fe(II)	85.5	85.5	91.1
	0.47	0.65	octahedral clay−Fe(III)	14.5		

[a] All spectra were collected at T = 85 °K. CS = center shift, QS = quadrupole split, and RA = relative phase abundance in %. Site assignments were done comparing the fitted hyperfine parameters to known ranges for clay−Fe (http://www.amazon.com/Mössbauer-Spectroscopy-Environmental-Industrial-Utilization/dp/1402077262).

nitrobenzene reduction due to the formation and reaction of clay-Fe(II).

Prior work has shown that biological and chemical reduction of clay minerals can yield spectroscopically different clay mineral products—as determined by Mössbauer spectra collected at 4 °C.[40] Here we used Mössbauer spectroscopy at 85 °K to compare biologically- and chemically reduced specimens of SWy-2 and NAu-2 (Figure 2). Characterization of both minerals in their native redox-state indicated that both minerals contained only Fe(III), within detection limits (∼1%). SWy-2 contained only octahedrally coordinated Fe(III) while NAu-2 contained mostly octahedral Fe(III) (96%) with a small amount of tetrahedral Fe(III) (4%). The spectra were consistent with previously published data.[4] For SWy-2, the biologically- and chemically reduced specimens were virtually identical, containing both octahedral Fe(III) and octahedral Fe(II) (Figure 2, left: B,D). The slight differences in relative areas of the Fe(II) and Fe(III) doublets can be attributed to challenges in controlling the extent of reduction using dithionite. For NAu-2, however, spectral variations were observed, particularly for the structural Fe(II) (Figure 2, right: B,C). The spectrum of biologically reduced NAu-2 was best fit using two Fe(II) doublets, both characteristic of octahedral Fe(II) in a clay mineral.[48,49] The spectrum of chemically reduced NAu-2 was best fit using only one Fe(II) doublet, suggesting that the local binding environment of Fe(II) in NAu-2 varied between the two reduced samples.

Even though it is difficult to correlate spectroscopic differences to reactivity[50] (e.g., since coexisting factors can influence fit parameters[51−55]), we found that chemically reduced iron-bearing clay minerals reduced nitrobenzene more rapidly than biologically reduced iron-bearing clay minerals (Figure 3, Table 3). At near-equal clay−Fe(II) concentrations and essentially equal reduction extents, dithionite-reduced SWy-2 [1.1 mM clay−Fe(II), 91% Fe(II)] reduced nitrobenzene faster (k_{clay} = 0.0117 d^{-1}, R_{NB} = 0.680 μeq L^{-1} h^{-1}) as compared to biologically reduced SWy-2 (1.3 mM clay−Fe(II), 90% Fe(II);

k_{clay} = 0.00770 d^{-1}, R_{NB} = 0.324 μeq L^{-1} h^{-1}). Similar results were obtained with NAu-2. At near-equal clay−Fe(II) concentrations and reduction extents, dithionite-reduced NAu-2 (5.1 mM clay−Fe(II), 38% Fe(II), 3.3 g L^{-1}) reduced nitrobenzene faster (k_{clay} = 0.0934 d^{-1}, R_{NB} = 3.41 μeq L^{-1} h^{-1}) as compared to biologically reduced NAu-2 (5.3 mM clay-Fe(II), 35% Fe(II), 3.7 g L^{-1}; k_{clay} = 0.0326 d^{-1}, R_{NB} = 1.79 μeq L^{-1} h^{-1}).

We also found that chemically reduced NAu-2 reduced nitrobenzene faster as compared to chemically reduced SWy-2 (Table 3). Because SWy-2 (0.40 mmol Fe/g) and NAu-2 (4.1 mmol Fe/g) contain different amounts of Fe and are biologically reduced to different extents, abiotic experiments were conducted with clay minerals that had been chemically reduced to the same extent. At equal clay-Fe(II) concentrations [1.1 mM clay-Fe(II)] and equal reduction extents [91% Fe(II)], dithionite-reduced NAu-2 reduced nitrobenzene faster (k_{clay} = 0.0139 d^{-1}, R_{NB} = 0.757 μeq L^{-1} h^{-1} ; Table 3) as compared to dithionite-reduced SWy-2 (k_{clay} = 0.0117 d^{-1}, R_{NB} = 0.680 μeq L^{-1} h^{-1} ; Table 3). The faster nitrobenzene reduction kinetics were measured even with a 10-fold lower clay suspension used with the dithionite-reduced NAu-2 (0.31 g/L) as compared to dithionite-reduced SWy-2 (3.1 g/L). The different reactivity of SWy-2 versus NAu-2 may have been caused by the different types of structural Fe(II) in these clay minerals (Table 2).[22,37]

The different reactivity of SWy-2 versus NAu-2 toward nitrobenzene may also have been caused by the different reduction potentials (E_h) of these clay minerals. Recently, our group developed a mediated electrochemical technique to measure reduction potential values for structural Fe in clay minerals as a function of Fe(II)/Total$_{Fe}$.[4,50] These measurements provided the redox profile distributions to relate the percentage of structural Fe(II) to E_h.[50] From the redox profile distributions for SWy-2 and NAu-2, we found that 91% Fe(II) dithionite-reduced NAu-2 has a more negative reduction potential (E_h ≈ −0.53 V) than 91% Fe(II) dithionite-reduced SWy-2
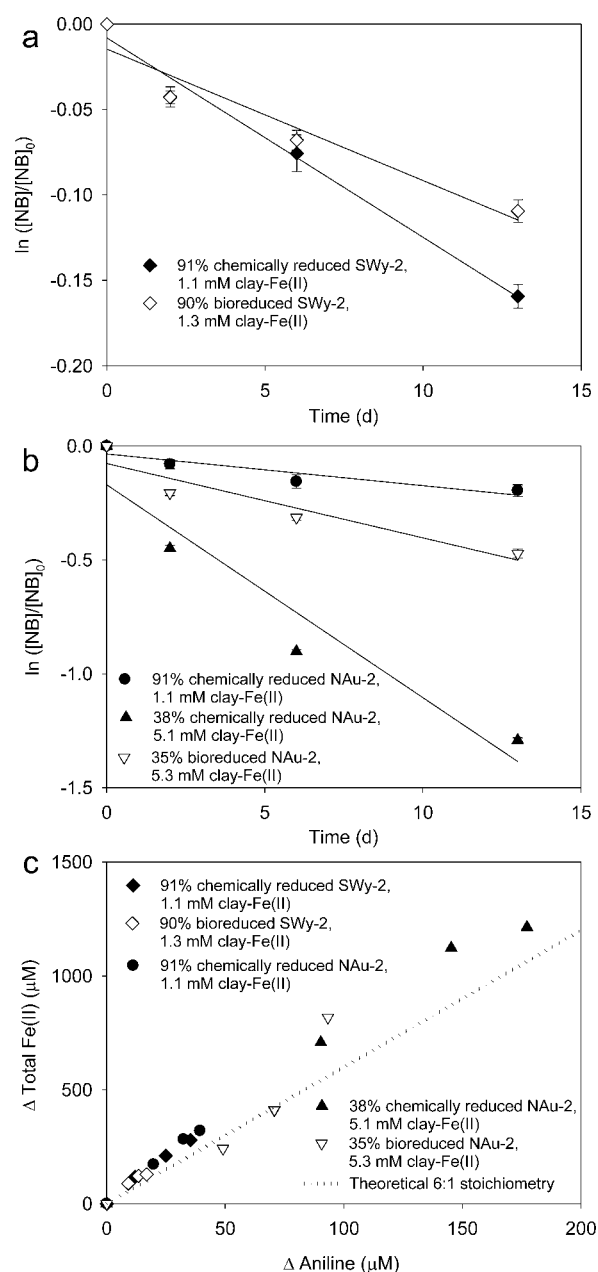
Figure 3. Abiotic reduction of nitrobenzene by biologically reduced and chemically reduced iron-bearing clay minerals. (a) Montmorillonite SWy-2. (b) Nontronite NAu-2. (c) Stoichiometric relationships between Δ mol Fe(II) and Δ mol aniline for the different clay-Fe(II) measurements. Dashed line represents theoretical stoichiometry of 6 Δ mol Fe(II) to 1 Δ mol aniline.

($E_h \approx -0.29$ V). Our results imply that the E_h of iron-bearing clay minerals may influence their reaction rates with NACs.

Environmental Significance. We believe this is the first study demonstrating that iron-bearing clay minerals can enhance the bioreduction of nitrobenzene. In our previous study with hematite, nitrobenzene and DMRB, we showed that hematite could enhance the bioreduction of nitrobenzene.[35] Incubations periods in that study were relatively short (<24 h) such that direct bacterial reduction of nitrobenzene was far more important than indirect reduction by biogenic Fe(II). In our current study, however, we show that indirect contaminant reduction by biogenic clay–Fe(II) becomes much more important as the incubation period increases (>500 h). The reactivity in these long-term incubations may better represent environmental systems that have been reduced slowly and for a long time (e.g., aquifers contaminated with organic pollutants). While Fe(II) produced via bioreduction of Fe(III) oxides may be transported out of an aquifer, biogenic clay–Fe(II) would remain as an important redox-active component.

We also believe this is the first study demonstrating that biologically reduced iron-bearing clay minerals are less reactive than chemically reduced iron-bearing clay minerals toward nitrobenzene. While the reason for this difference is unresolved, it is consistent with spectroscopic studies showing structural differences that depend upon the reduction pathway[40] and with our own Mössbauer spectroscopy results (Figure 2, Table 2). A companion study has been completed to characterize the reactivity of biologically reduced iron-bearing clay minerals toward NACs.[56] Because most contaminated aquifers become reduced via biological activity, the reactivity of biogenic clay-Fe(II) toward reducible contaminants is particularly important.

ASSOCIATED CONTENT

Ⓢ Supporting Information

Figure S1. Bioreduction of Fe-bearing clay minerals by *Shewanella putrefaciens* CN32 in the presence of aniline or methanol. Figure S2. Pseudo-first-order reduction rates during bioreduction of nitrobenzene in the presence of NAu-2, SWy-2 and Al₂O₃. Figure S3. Analytical interference of clay-Fe(II) measurement by nitrosobenzene. This material is available free of charge via the Internet at http://pubs.acs.org.

AUTHOR INFORMATION

Corresponding Author
*William D. Burgos, Dept. of Civil and Environmental Engineering, The Pennsylvania State University, 212 Sackett Building, University Park, PA, 16802 phone: 814-863-0578; fax: 814-863-7304. Email: wdb3@psu.edu.

Table 3. Summary of Pseudo-First-Order Rate Constants and Zero-Order Rates for the Abiotic Reduction of Nitrobenzene by Biologically-Reduced or Chemically-Reduced Montmorillonite SWy-2 or Nontronite NAu-2.[a]

clay–Fe(II) description	SWy-2 (g L⁻¹)/clay-Fe(II) (mM)	NAu-2 (g L⁻¹)/clay-Fe(II) (mM)	first-order rate constant k_{clay} (d⁻¹)[b] (R^2)[c]	zero-order rate R_{NB} (μeq L⁻¹ h⁻¹)
90% biologically reduced SWy-2	3.6/1.3	0/0	0.00770 ± 0.0004 (0.928)	0.324
91% chemically reduced SWy-2	3.1/1.1	0/0	0.0117 ± 0.002 (0.986)	0.680
35% biologically reduced NAu-2	0/0	3.7/5.3	0.0326 ± 0.001 (0.893)	1.79
38% chemically reduced NAu-2	0/0	3.3/5.1	0.0934 ± 0.003 (0.920)	3.41
91% chemically reduced NAu-2	0/0	0.31/1.1	0.0139 ± 0.001 (0.852)	0.757

[a]All experiments conducted with [nitrobenzene]$_0$ = 250 μM in 50 mM PIPES, pH 6.8. [b]Regression slope ±95% confidence interval. [c]R^2 for regression of ln ([NB]$_t$/[NB]$_0$) versus time (0–13 d).

■ REFERENCES

(1) Favre, F.; Stucki, J. W.; Boivin, P. Redox properties of structural Fe in ferruginous smectite. A discussion of the standard potential and its environmental implications. *Clays Clay Miner.* **2006**, *54* (4), 466−472.

(2) Stucki, J. W.; Lee, K.; Goodman, B. A.; Kostka, J. E. Effects of in situ biostimulation on iron mineral speciation in a sub-surface soil. *Geochim. Cosmochim. Acta* **2007**, *71* (4), 835−843.

(3) Komlos, J.; Peacock, A.; Kukkadapu, R. K.; Jaffe, P. R. Long-term dynamics of uranium reduction/reoxidation under low sulfate conditions. *Geochim. Cosmochim. Acta* **2008**, *72* (15), 3603−3615.

(4) Gorski, C. A.; Aeschbacher, M.; Soltermann, D.; Voegelin, A.; Baeyens, B.; Fernandes, M. M.; Hofstetter, T. B.; Sander, M. Redox properties of structural Fe in clay minerals. 1. Electrochemical quantification of electron-donating and -accepting capacities of smectites. *Environ. Sci. Technol.* **2012**, *46* (17), 9360−9368.

(5) Coughlin, B. R.; Stone, A. T. Nonreversible adsorption of divalent metal-Ions (Mn-II, Co-II Ni-II Cu-II and Pb-II) onto goethite—Effects of acidification, Fe-II Addition, and picolinic-acid addition. *Environ. Sci. Technol.* **1995**, *29* (9), 2445−2455.

(6) Jenne, E. A. Controls on Mn Fe Co Ni Cu and Zn concentrations in soils and water - significant role of hydrous Mn and Fe oxides. *Adv. Chem. Ser.* **1968**, *73*, 337−387.

(7) Lovley, D. R. Microbial Fe(III) reduction in subsurface environments. *Fems Microbiol. Rev.* **1997**, *20* (3−4), 305−313.

(8) Jickells, T. D.; An, Z. S.; Andersen, K. K.; Baker, A. R.; Bergametti, G.; Brooks, N.; Cao, J. J.; Boyd, P. W.; Duce, R. A.; Hunter, K. A.; Kawahata, H.; Kubilay, N.; laRoche, J.; Liss, P. S.; Mahowald, N.; Prospero, J. M.; Ridgwell, A. J.; Tegen, I.; Torres, R. Global iron connections between desert dust, ocean biogeochemistry, and climate. *Science* **2005**, *308* (5718), 67−71.

(9) Pollard, R. T.; Salter, I.; Sanders, R. J.; Lucas, M. I.; Moore, C. M.; Mills, R. A.; Statham, P. J.; Allen, J. T.; Baker, A. R.; Bakker, D. C. E.; Charette, M. A.; Fielding, S.; Fones, G. R.; French, M.; Hickman, A. E.; Holland, R. J.; Hughes, J. A.; Jickells, T. D.; Lampitt, R. S.; Morris, P. J.; Nedelec, F. H.; Nielsdottir, M.; Planquette, H.; Popova, E. E.; Poulton, A. J.; Read, J. F.; Seeyave, S.; Smith, T.; Stinchcombe, M.; Taylor, S.; Thomalla, S.; Venables, H. J.; Williamson, R.; Zubkov, M. V. Southern Ocean deep-water carbon export enhanced by natural iron fertilization. *Nature* **2009**, *457* (7229), 577−U581.

(10) Eglinton, T. I. Geochemistry A rusty carbon sink. *Nature* **2012**, *483* (7388), 165−166.

(11) Lalonde, K.; Mucci, A.; Ouellet, A.; Gelinas, Y. Preservation of organic matter in sediments promoted by iron. *Nature* **2012**, *483* (7388), 198−200.

(12) Riedel, T.; Zak, D.; Biester, H.; Dittmar, T. Iron traps terrestrially derived dissolved organic matter at redox interfaces. *Proc. Natl. Acad. Sci. U. S. A.* **2013**, *110* (25), 10101−10105.

(13) Borch, T.; Kretzschmar, R.; Kappler, A.; Van Cappellen, P.; Ginder-Vogel, M.; Voegelin, A.; Campbell, K. Biogeochemical redox processes and their impact on contaminant dynamics. *Environ. Sci. Technol.* **2010**, *44* (1), 15−23.

(14) Elsner, M.; Schwarzenbach, R. P.; Haderlein, S. B. Reactivity of Fe(II)-bearing minerals toward reductive transformation of organic contaminants. *Environ. Sci. Technol.* **2004**, *38* (3), 799−807.

(15) Gates, W. P.; Bouazza, A. Churchman G.J. Bentonite clay keeps pollutants at bay. *Elements* **2009**, *5* (2), 105−110.

(16) Anastacio, A. S.; Aouad, A.; Sellin, P.; Fabris, J. D.; Bergaya, F.; Stucki, J. W. Characterization of a redox-modified clay mineral with respect to its suitability as a barrier in radioactive waste confinement. *Appl. Clay Sci.* **2008**, *39* (3−4), 172−179.

(17) Bishop, M. E.; Glasser, P.; Dong, H. L.; Arey, B.; Kovarik, L. Reduction and immobilization of hexavalent chromium by Fe-bearing clay minerals. *Abstr. Pap. Am. Chem. Soc.* **2013**, *246*.

(18) Brigatti, M. F.; Franchini, G.; Lugli, C.; Medici, L.; Poppi, L.; Turci, E. Interaction between aqueous chromium solutions and layer silicates. *Appl. Geochem.* **2000**, *15* (9), 1307−1316.

(19) Fredrickson, J. K.; Zachara, J. M.; Kennedy, D. W.; Kukkadapu, R. K.; McKinley, J. P.; Heald, S. M.; Liu, C. X.; Plymale, A. E. Reduction of TcO_4^- by sediment-associated biogenic Fe(II). *Geochim. Cosmochim. Acta* **2004**, *68* (15), 3171−3187.

(20) Bishop, M. E.; Dong, H. L.; Kukkadapu, R. K.; Liu, C. X.; Edelmann, R. E. Bioreduction of Fe-bearing clay minerals and their reactivity toward pertechnetate (Tc-99). *Geochim. Cosmochim. Acta* **2011**, *75* (18), 5229−5246.

(21) Yang, J. J.; Kukkadapu, R. K.; Dong, H. L.; Shelobolina, E. S.; Zhang, J.; Kim, J. Effects of redox cycling of iron in nontronite on reduction of technetium. *Chem. Geol.* **2012**, *291*, 206−216.

(22) Neumann, A.; Hofstetter, T. B.; Lussi, M.; Cirpka, O. A.; Petit, S.; Schwarzenbach, R. P. Assessing the redox reactivity of structural iron in smectites using nitroaromatic compounds as kinetic probes. *Environ. Sci. Technol.* **2008**, *42* (22), 8381−8387.

(23) Hofstetter, T. B.; Neumann, A.; Schwarzenbach, R. P. Reduction of nitroaromatic compounds by Fe(II) species associated with iron-rich smectites. *Environ. Sci. Technol.* **2006**, *40* (1), 235−242.

(24) Hofstetter, T. B.; Schwarzenbach, R. P.; Haderlein, S. B. Reactivity of Fe(II) species associated with clay minerals. *Environ. Sci. Technol.* **2003**, *37* (3), 519−528.

(25) Neumann, A.; Hofstetter, T. B.; Skarpeli-Liati, M.; Schwarzenbach, R. P. Reduction of polychlorinated ethanes and carbon tetrachloride by structural Fe(II) in smectites. *Environ. Sci. Technol.* **2009**, *43* (11), 4082−4089.

(26) Schaefer, M. V.; Gorski, C. A.; Scherer, M. M. Spectroscopic evidence for interfacial Fe(II)-Fe(III) electron transfer in a clay mineral. *Environ. Sci. Technol.* **2011**, *45* (2), 540−545.

(27) Gan, H.; Stucki, J. W.; Bailey, G. W. Reduction of structural Iron in ferruginous smectite by free-radicals. *Clays Clay Miner.* **1992**, *40* (6), 659−665.

(28) Pentrakova, L.; Su, K.; Pentrak, M.; Stuck, J. W. A review of microbial redox interactions with structural Fe in clay minerals. *Clay Miner.* **2013**, *48* (3), 543−560.

(29) Dong, H. L.; Jaisi, D. P.; Kim, J.; Zhang, G. X. Microbe-clay mineral interactions. *Am. Mineral.* **2009**, *94* (11−12), 1505−1519.

(30) Padda, R. S.; Wang, C. Y.; Hughes, J. B.; Kutty, R.; Bennett, G. N. Mutagenicity of nitroaromatic degradation compounds. *Environ. Toxicol. Chem.* **2003**, *22* (10), 2293−2297.

(31) Purohit, V.; Basu, A. K. Mutagenicity of nitroaromatic compounds. *Chem. Res. Toxicol.* **2000**, *13* (8), 673−692.

(32) Luan, F. B.; Burgos, W. D.; Xie, L.; Zhou, Q. Bioreduction of nitrobenzene, natural organic matter, and hematite by *Shewanella putrefaciens* CN32. *Environ. Sci. Technol.* **2010**, *44* (1), 184−190.

(33) Zhu, Z. K.; Tao, L.; Li, F. B. 2-Nitrophenol reduction promoted by *S. putrefaciens* 200 and biogenic ferrous iron: The role of different size-fractions of dissolved organic matter. *J. Hazard. Mater.* **2014**, *279*, 436−443.

(34) Luan, F.b.; Gorski, C. A.; Burgos, W. D. Thermodynamic controls on the microbial reduction of iron-bearing nontronite and uranium. *Environ. Sci. Technol.* **2014**, *48* (5), 2750−2758.

(35) Zhang, G. X.; Senko, J. M.; Kelly, S. D.; Tan, H.; Kemner, K. M.; Burgos, W. D. Microbial reduction of iron(III)-rich nontronite and uranium(VI). *Geochim. Cosmochim. Acta* **2009**, *73* (12), 3523−3538.

(36) McAllister, L. E.; Semple, K. T., Role of clay and organic matter in the biodegradation of organics in soil. In *Geomicrobiology: Molecular and Environmental Perspective*; Springer-Verlag: Berlin, Berlin, 2010; pp 367−384.

(37) Neumann, A.; Petit, S.; Hofstetter, T. B. Evaluation of redox-active iron sites in smectites using middle and near infrared spectroscopy. *Geochim. Cosmochim. Acta* **2011**, *75* (9), 2336−2355.

644 (38) Gorski, C. A.; Scherer, M. M. *Fe²⁺ Sorption at the Fe Oxide-Water*
645 *Interface: A Revised Conceptual Framework, Aquatic Redox Chemistry*;
646 American Chemical Society: WA, 2011; pp 315−343.
647 (39) Ernstsen, V.; Gates, W. P.; Stucki, J. W. Microbial reduction of
648 structural iron in clays—A renewable source of reduction capacity. *J.*
649 *Environ. Qual.* **1998**, *27* (4), 761−766.
650 (40) Ribeiro, F. R.; Fabris, J. D.; Kostka, J. E.; Komadel, P.; Stucki, J.
651 W. Comparisons of structural iron reduction in smectites by bacteria
652 and dithionite: II. A variable-temperature Mossbauer spectroscopic
653 study of Garfield nontronite. *Pure Appl. Chem.* **2009**, *81* (8), 1499−
654 1509.
655 (41) Royer, R. A.; Burgos, W. D.; Fisher, A. S.; Unz, R. F.; Dempsey,
656 B. A. Enhancement of biological reduction of hematite by electron
657 shuttling and Fe(II) complexation. *Environ. Sci. Technol.* **2002**, *36* (9),
658 1939−1946.
659 (42) Keeling, J. L.; Raven, M. D.; Gates, W. P. Geology and
660 characterization of two hydrothermal nontronites from weathered
661 metamorphic rocks at the Uley Graphite Mine, South Australia. *Clay*
662 *Clay Miner.* **2000**, *48* (5), 537−548.
663 (43) Luan, F. B.; Burgos, W. D. Sequential extraction method for
664 determination of Fe(II/III) and U(IV/VI) in suspensions of iron-
665 bearing phyllosilicates and uranium. *Environ. Sci. Technol.* **2012**, *46*
666 (21), 11995−12002.
667 (44) Stucki, J. W.; Golden, D. C.; Roth, C. B. Preparation and
668 handling of dithionite-reduced smectite suspensions. *Clay Clay Min.*
669 **1984**, *32* (3), 191−197.
670 (45) Jaisi, D. P.; Dong, H. L.; Liu, C. X. Influence of biogenic Fe(II)
671 on the extent of microbial reduction of Fe(III) in clay minerals
672 nontronite, Illite, and chlorite. *Geochim. Cosmochim. Acta* **2007**, *71* (5),
673 1145−1158.
674 (46) Stookey, L. L. Ferrozine—A new spectrophotometric reagent
675 for iron. *Anal. Chem.* **1970**, *42* (7), 779−781.
676 (47) Klausen, J.; Trober, S. P.; Haderlein, S. B.; Schwarzenbach, R. P.
677 Reduction of substituted nitrobenzenes by Fe(II) in aqueous mineral
678 suspensions. *Environ. Sci. Technol.* **1995**, *29* (9), 2396−2404.
679 (48) Murad, E.; Cashion, J. *Mössbauer Spectroscopy of Environmental*
680 *Materials and Their Industrial Utilization*; Kluwer Academic Publishers:
681 Dordrecht, 2006.
682 (49) McCammon, C. Mössbauer spectroscopy of minerals. In
683 *Mineral Physics and Crystallography: A Handbook of Physical Constants*;
684 American Geophysical Union: Washington, D. C., 1995.
685 (50) Gorski, C. A.; Klupfel, L. E.; Voegelin, A.; Sander, M.;
686 Hofstetter, T. B. Redox properties of structural Fe in clay minerals: 3.
687 Relationships between smectite redox and structural properties.
688 *Environ. Sci. Technol.* **2013**, *47* (23), 13477−13485.
689 (51) Dyar, M. D.; Agresti, D. G.; Schaefer, M. W.; Grant, C. A.;
690 Sklute, E. C., Mossbauer spectroscopy of earth and planetary materials.
691 In *Annual Review of Earth and Planetary Sciences*; Annual Reviews: Palo
692 Alto, 2006; pp 83−125.
693 (52) Evans, R. J.; Rancourt, D. G.; Grodzicki, M. Hyperfine electric
694 field gradients and local distortion environments of octahedrally
695 coordinated Fe²⁺. *Am. Mineral.* **2005**, *90* (1), 187−198.
696 (53) Evans, R. J.; Rancourt, D. G.; Grodzicki, M. Hyperfine electric
697 field gradient tensors at Fe²⁺ sites in octahedral layers: Toward
698 understanding oriented single-crystal Mössbauer spectroscopy meas-
699 urements of micas. *Am. Mineral.* **2005**, *90* (10), 1540−1555.
700 (54) Rancourt, D. G. Mössbauer spectroscopy in clay sciences.
701 *Hyperfine Interact.* **1998**, *117* (1−4), U7−U8.
702 (55) Cashion, J. D.; Gates, W. P.; Thomson, A. Mossbauer and IR
703 analysis of iron sites in four ferruginous smectites. *Clay Miner.* **2008**,
704 *43* (1), 83−93.
705 (56) Luan, F. B.; Gorski, C. A.; Burgos, W. D. Linear free energy
706 relationships for the biotic and abiotic reduction of nitroaromatic
707 compounds. *Environ. Sci. Technol.* **2014**, submitted.